Ultrahigh Sensitive Piezotronic Strain Sensors Based on a $ZnSnO_3$ Nanowire/Microwire

Jyh Ming Wu,[†,‡] Cheng-Ying Chen,[†,⊥] Yan Zhang,[†] Kuan-Hsueh Chen,[‡] Ya Yang,[†] Youfan Hu,[†] Jr-Hau He,[⊥] and Zhong Lin Wang[†,§,*]

[†]School of Materials Science and Engineering, Georgia Institute of Technology, Atlanta, Georgia 30332, United States, [‡]Department of Materials Science and Engineering, Feng Chia University, Taichung 40724, Taiwan, [§]Beijing Institute of Nanoenergy and Nanosystems, Chinese Academy of Sciences, Beijing, China, and [⊥]Institute of Photonics and Optoelectronics and Department of Electrical Engineering, National Taiwan University, Taipei, 10617 Taiwan

ABSTRACT

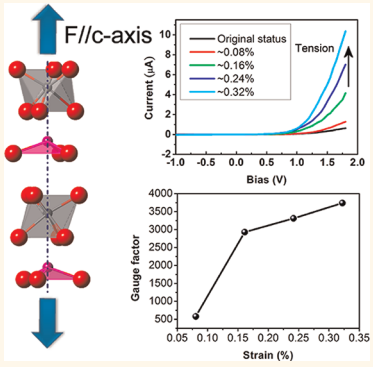

We demonstrated a flexible strain sensor based on $ZnSnO_3$ nanowires/microwires for the first time. High-resolution transmission electron microscopy indicates that the $ZnSnO_3$ belongs to a rhombohedral structure with an *R3c* space group and is grown along the [001] axis. On the basis of our experimental observation and theoretical calculation, the characteristic *I*–*V* curves of $ZnSnO_3$ revealed that our strain sensors had ultrahigh sensitivity, which is attributed to the piezopotential-modulated change in Schottky barrier height (SBH), that is, the piezotronic effect. The on/off ratio of our device is ~587, and a gauge factor of 3740 has been demonstrated, which is 19 times higher than that of Si and three times higher than those of carbon nanotubes and ZnO nanowires.

KEYWORDS: $ZnSnO_3$ · nanowires/microwires · strain sensor · flexible · gauge factor

In the noncentrosymmetric (NCS) oxide group, ferroelectric perovskites containing Pb^{2+} and Bi^{3+} exhibit high polarization and piezoelectric performance, and the new Pb- and Bi-based perovskites have recently attracted considerable attention as ferroelectric and multiferroic oxide candidates.[1,2] However, when considering lead toxicity, lead-free materials would be more environmentally benign and suitable for a wide range of biological applications.[3] It is therefore becoming increasingly essential to develop high-performance, lead-free, piezoelectric materials. In the past decade, ZnO is one of the most interesting functional lead-free-based materials because of its outstanding piezoelectric effect.[4] Therefore, a large number of multifunctional ZnO nanowire/microwire devices have extensively been demonstrated in piezotronic devices[5] such as piezoelectric field effect transistors,[6] solar cells,[7] piezoelectric diodes,[8] nanogenerators,[9] piezoelectric strain sensors,[10] and biological sensors, *etc.*[3]

Lead-free-based materials are increasingly interesting for medical imaging and underwater applications due to low acoustical impedance.[11] However, many lead-free piezoelectric materials in the NCS group still remain undiscovered. Among NCS oxides, special attention has been paid to the $LiNbO_3$ (LN)-type structure with the space group of *R3c* due to its large polarization along the *c*-axis. However, the studies of LN-type $ZnSnO_3$ structures are mainly focused on the electronic structure,[12,13] spontaneous polarization,[14] piezoelectric, and nonlinear optical behaviors[15] based on the density functional theory.[16] Although the rhombohedral crystal structure with *R3c* space group of $ZnSnO_3$ exhibits piezoelectric properties, it has not been as extensively investigated as lead zirconate titanate[17] (PZT) in piezoelectric sensors and actuators. Inaguma[18] reported that the calculated value of polarization in $ZnSnO_3$ along the *c*-axis is 59 $\mu C\,cm^{-2}$,[18] which is much larger than that of ZnO, ~5 $\mu C\,cm^{-2}$.[19,20] Thus, it is interesting to investigate the performance of $ZnSnO_3$ nanowires/microwires in terms of the piezopotential distribution along the *c*-axis and practical application in the piezotronic strain sensor.

In this work, we first introduce a new type of strain sensor based on $ZnSnO_3$

* Address correspondence to zlwang@gatech.edu.

Received for review March 9, 2012 and accepted April 7, 2012.

Published online April 07, 2012
10.1021/nn3010558

nanowires/microwires. Due to the obvious change in Schottky barrier height (SBH) under a small variation of compressive and tensile strain, the characteristic $I-V$ curves of the strain sensor were significantly modulated. Our theoretical calculation presents that the piezopotential distribution along the c-axis for $ZnSnO_3$ nanowire/microwire is $\pm$86 V, which has a positive or negative sign depending on whether the microwire is under tensile or compressive strain, respectively.[5] Our experimental observation and theoretical calculation present that the characteristic $I-V$ curves in $ZnSnO_3$ microwires are significantly tuning by the external applied strain.[10,21] In addition, a gauge factor as high as 3740 was received from the $ZnSnO_3$ strain sensor. The result is 19 times and three times higher than that of Si and ZnO nanowires (or carbon nanotubes), respectively.

RESULTS AND DISCUSSION

The detailed growth method of our nanowires/microwires is given in the Experimental Methods. Figure 1a shows a scanning electron microscopy (SEM) image of the as-grown nanowires. The diameter and the length of the wires is less than 100 nm and up to hundreds of micrometers, respectively. To identify the crystal structure of $ZnSnO_3$, an individual nanowire with corresponding high-resolution transmission electron microscopy (HRTEM) images are shown in Figure 1b,c, respectively. Combining the HRTEM image with the selected area diffraction (SAD) pattern (see Figure 1d) revealed that the growth direction of the nanowire is [001]. In this case, the SAD pattern was further indexed to a rhombohedral structure of $R3c$ space group with lattice constants of $a = b = 0.52622$ nm and $c = 1.40026$ nm. Figure 1e shows a schematic diagram and optical image of a fabricated strain sensor based on a single $ZnSnO_3$ microwire. Silver paste was applied at both ends of the wire to fix its two ends securely on a flexible polystyrene (PS) substrate. The substrate has a length of ~40 mm, width of ~10 mm, and thickness of 1 mm.

To understand the crystallographic structure of $ZnSnO_3$, the crystal structure of the $ZnSnO_3$ with $R3c$ space group is shown in Figure 2a, which consisted of two octahedra frameworks of ZnO_6 and SnO_6. In addition to the ZnO_6 octahedron sharing a face with the SnO_6 octahedron, the crystal structure presents that each Zn octahedron shares corners with another Zn octahedron, and each Sn octahedron shares corners with another Sn octahedral structure.[18] The Zn and Sn ion reside at a nonquivalent in the octahedral structure of ZnO_6 and SnO_6, respectively. To indicate the displacement of Zn and Sn ions in octahedral structures of ZnO_6 and SnO_6, respectively, a perspective crystal structure of $ZnSnO_3$ is further shown in Figure 2b. The ZnO_6 octahedron has three short bonds of 0.2041 nm and three long bonds of 0.2308 nm. The SnO_6 octahedron has three short bonds of 0.2008 nm and three long bonds of 0.2094 nm.[18] Figure 2b shows

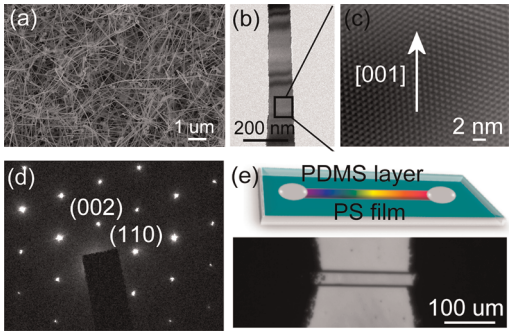

Figure 1. (a) Top-view image of $ZnSnO_3$ nanowires. (b) Individual $ZnSnO_3$ nanowire. (c) Corresponding high-resolution transmission electron microscopy image. (d) Corresponding SAD pattern revealing the nanowire's growth direction of [001]. (e) Schematic diagram and optical microscopy image of a single $ZnSnO_3$-based strain sensor.

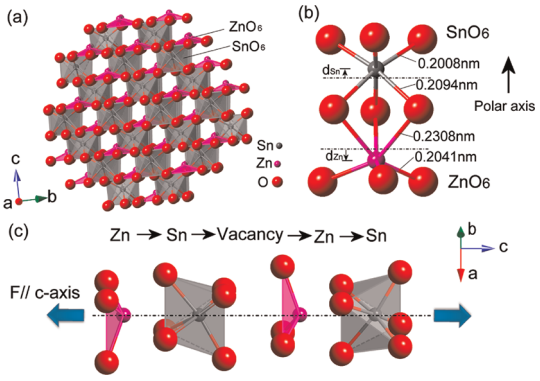

Figure 2. (a) Atomic model of the rhombohedral structure $ZnSnO_3$. (b) Deviation of Zn (d_{zn}) and Sn (d_{Sn}) ions at nonequivalent positions in the octahedral ZnO_6 and SnO_6, respectively. (c) Crystal structure of $ZnSnO_3$ from the perspective of the octahedral framework, the cation sequence is Zn−Sn−vacancy−Zn−Sn along the c-axis (from left to right).

that the calculated displacement of Zn (d_{zn}) and Sn (d_{sn}) ions in ZnO_6 and SnO_6 octahedron is around 0.05 and 0.02 nm, respectively. Figure 2c shows that the cation sequence is Zn−Sn−vacancy−Zn−Sn−vacancy (from left to right) and is aligned along the c-axis. Therefore, $ZnSnO_3$ structure has Zn and Sn in unequivalent cation positions along the c-axis when a tensile or compressive force (F) is applied in parallel (see Figure 2c), causing the ionic charges to polar along the c-axis. These dipoles are oriented on the c-axis such that the extended structure exhibits a polar moment along the same direction.[22]

The applied strain to the single $ZnSnO_3$ microwire can be estimated according to our previous work (see Supporting Information S1).[10] Since the dimension of $ZnSnO_3$ microwire is small, the mechanical behavior of the plastic substrate was not affected by the microwire. Therefore, the external strain applied on the $ZnSnO_3$ microwire was only considered pure tension or compressive strain along the c-axis. As a simple estimation of the strain, the microwire can be evaluated by using the Saint-Venant bending theory.[23] Therefore, the compressive and

tensile strains in this work were calculated as 0, ±0.08, and ±0.24%. The positive or negative sign depends on whether tensile or compressive strain was applied to the microwire, respectively.

To investigate how strain affects the electrical transport property ($I-V$) of $ZnSnO_3$ microwire-based devices, strain-dependent $I-V$ characteristics were measured, as shown in Figure 3a. The $I-V$ curves show excellent rectification behavior under all strain conditions, indicating the existence of two Schottky barriers at the interface with unequal barrier heights. In the positive bias range, the current of the device (device no. 1) increased and decreased with tensile and compressive strain, respectively. The $I-V$ curves could be fully recovered as the strains were released.

The presence of a Schottky barrier at the interface of the metal and semiconductor is an important factor in determining electrical transport properties of the metal−semiconductor−metal (M−S−M) structure in the devices. To understand the asymmetric $I-V$ curves in Figure 3a, the energy band diagram with back-to-back Schottky barriers was proposed, as shown in Figure 3b. Here we assume that the SBH at the drain side (Φ_d) is higher than that at the source side (Φ_s). If considering that nanowires/microwires had a low doping and impurity level, the dominant transport property at the barrier is thermionic emission and diffusion.[21] Thus, on the basis of the classic thermionic emission−diffusion theory (for $V \gg 3\ kT/q \sim 77$ mV) for a reversal bias voltage V and at temperature T, the current through the reversely biased Schottky barrier (Φ_s) is given as the following formula 1.

$$I = SA^{**}T^2 \exp\left(-\frac{\Phi_s}{kT}\right) \exp\left(\frac{\sqrt[4]{\frac{q^7 N_d \left(V + V_{bi} - \frac{kT}{q}\right)}{8\pi^2 \varepsilon_s^3}}}{kT}\right) \quad (1)$$

where S is the area of the source Schottky barrier, A^{**} is the effective Richardson constant, N_d is the donor impurity density, ε_s is the permittivity of $ZnSnO_3$, q is the electron charge, k is the Boltzmann constant, and V_{bi} is the potential at barrier. Figure 3c further indicates that the ln $I-V^{1/4}$ curve is almost linear. The Schottky barrier formula can precisely explain our experimental data. Therefore, we can use the model of strain-induced change in SBH (see Supporting Information S2) to further explain how the high sensitivity of SBH changes as a function of applied strain on the newly developed $ZnSnO_3$ microwires.

Figure 3d exhibits that the SBH was significantly changed as the device was subjected to various strain by fixing a bias voltage. By statistically analyzing the change of SBH at the biases of 1, 1.2, 1.5, and 2 V, the average change of SBH has an approximately linear relationship under a various strain. The error bars can be ascribed to standard deviation. On the basis of our previous report of ZnO microwires,[10] the change of SBH for $ZnSnO_3$ under strain can be regarded as a combination of band structure change (piezoresistance effect) and piezotronic effect (see Supporting Information S3). A slow change in conductivity of $ZnSnO_3$ is observed in Figure S1, which shows that when the strain sensor was stretched and held for about 2−3 s, the time-dependent decay of the current at a fixed strain was observed. This indicates that the contribution from the piezotronic effect is possibly time-dependent because of the charge-trapping effect by impurity or vacancy states in the $ZnSnO_3$ microwires. On the basis of our experimental results, we have discovered a similar phenomenon in newly developed $ZnSnO_3$ nanowires/microwires in that the Schottky barrier shifts under stress/strain due to band structure change and piezoelectric effects.[21] Our experimental results are in good agreement with previous works on GaN,[11] GaAs, and ZnO.[21]

To understand how the newly developed $ZnSnO_3$ microwires can produce such a significant change of barrier height under a small strain, the distribution of the piezopotential in a $ZnSnO_3$ microwire was calculated using the Lippman theory.[24] For simplicity, we first ignored the free carrier effect (*i.e.*, doping effect or impurity level) in $ZnSnO_3$ microwires, so that the microwires are assumed to be an insulator to semiquantitatively comprehend their piezopotential distribution. The material constants of $ZnSnO_3$ used for the theoretical calculation were elastic constants.[25] When the microwire was bonded on the PS substrate and applied under tensile and compressive strain, the corresponding piezopotential distribution exhibited −86 V (see Figure 4a) and +86 V (see Figure 4b), respectively. It should be noted that the actual piezopotential in $ZnSnO_3$ is much lower than the calculated value due to the screening effect of the free charge carriers and finite conductance.[26,27] Using a piezoelectric $ZnSnO_3$ nanowire/microwire, the results indeed demonstrate the piezotronic theory in which, for a one-end stationary free-standing nanowire/microwire that is transversely pushed by an external force, the stretched side and the compressed side surfaces exhibit a negative and positive piezopotential, respectively. The piezopotential can then act as a transverse voltage for gating the charge transport along the nanowire/microwire.[28] Our experimental data and theoretical calculation demonstrate for the first time that the lead-free $ZnSnO_3$ nanomaterial exhibits an excellent piezoelectric response in the application of a strain sensor.

To practically understand the $ZnSnO_3$ microwire strain sensor application and its reliability, the device (device no. 2) was measured using repeated compressing

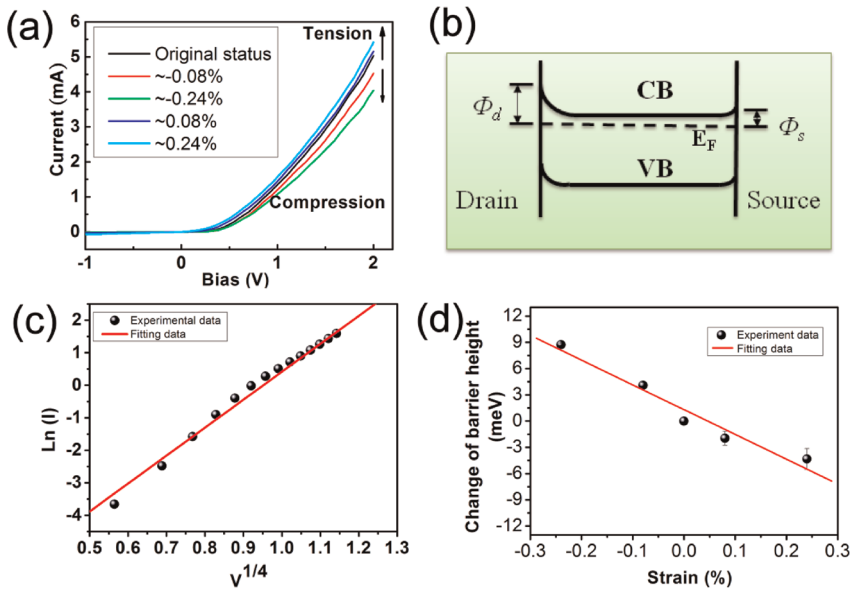

Figure 3. (a) *I*–*V* characteristic of a strain sensor at different strain. (b) Energy band diagram shows the asymmetric Schottky barrier heights at the source and drain contacts of a strain sensor. (c) Plot of ln *I* as a function $V^{1/4}$, using the data provided by the black line in (a). (d) Derived change in SBH as a function of strain, using the thermionic emission–diffusion model.

and stretching at a frequency of 0.2 Hz under a fixed bias of 2 V. Figure 5a shows that the responsive current from 256 nA increases to 152 μA under a tensile strain. Figure 5b presents that the responsive current from 256 nA decreases to 0.436 nA under a compressive strain. The current decreases with a compressive strain and increases with a tensile strain. The result is consistent with the *I*–*V* curve, as observed in Figure 3a. The on/off ratio of compressive and tensile strain is 587. This fact further demonstrates that a high sensitivity SBH change occurs in newly developed $ZnSnO_3$ microwires under various small strains. We found that the devices no. 1 and no. 2 exhibited a different piezopotential property. This can be ascribed to the screening effect of the free charge carriers,[26,27] which will accumulate and cause the piezoelectrical potential to be partially screened.[29] Therefore, the device exhibited a low sensitivity.

It is interesting to understand the performance of a strain sensor in practical applications. The gauge factor (GF) performance of an as-prepared strain sensor is further characterized by defining the ratio of relative change in electrical current (*I*) to the mechanical strain (ε, relative change in length), as given by eq 2.

$$GF = \delta I/I\varepsilon \qquad (2)$$

Figure 5d (device no. 3) shows that the highest gauge factor demonstrated in this work is 3740, indicating that the $ZnSnO_3$ microwires are an excellent candidate in strain sensor application. The result exceeds three times that of CNT or ZnO and is about 19 times higher than the Si strain sensor.

The SBH of a single $ZnSnO_3$ microwire can be modulated significantly under small strains and then exhibit a high gauge factor. This can be attributed to the piezotronic effect, in which a large spontaneous

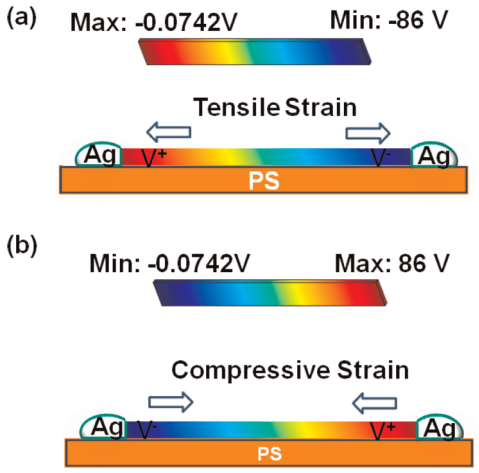

Figure 4. Numerical calculation of the piezoelectric potential distribution in a $ZnSnO_3$ microwire under axial strain of tension (a) and compression (b).

polarization effect naturally forms in the crystal structure along the *c*-axis due to the large displacement of Zn atoms,[25] creating an asymmetric effect positioned on the local contacts at the source and drain during the crystal growth process.[21,30] The calculated polarization of $ZnSnO_3$ is 59 μC cm^{-2},[31] which is 12 times higher than that of ZnO, ~5 μC cm^{-2}. Moreover, if considering the thin PDMS layer has much smaller Young's modulus of ~400–900 kpa than that of the PS substrate (~3–3.5 GPa), the PDMS layer will not affect the mechanical properties of the PS substrate at any significant level. Therefore, the SBH change in $ZnSnO_3$ microwires can be regarded as purely induced by the bending of the PS substrate at any direction. These may provide a reasonable explanation for how a high gauge factor was discovered in the $ZnSnO_3$ strain sensor.

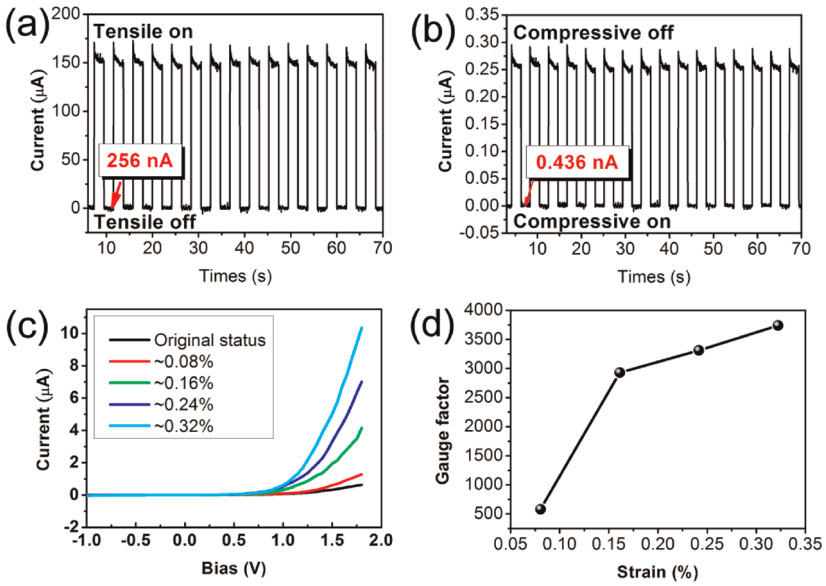

Figure 5. Current response of a strain sensor device (device no. 2) that was repeatedly applied under tension (a) and compression (b) at a frequency of 0.2 Hz under fixed bias of 2 V. (c) *I*–*V* characteristics of a strain sensor (device no. 3) under different strains. (d) Gauge factors derived from (c) as a function of various strains at 1.2 V.

CONCLUSION

We demonstrated for the first time that $ZnSnO_3$ microwires can be modulated by a variety strains. On the basis of our experimental observation and theoretical calculations, the $ZnSnO_3$ microwires exhibited an excellent piezotronic effect. The characteristic *I*–*V* curves exhibited ultrasensitivity to strains owing to the change in Schottky barrier height (SBH). The strain sensor exhibited a gauge factor as high as 3740, which is 19 times that of Si and three times that of carbon nanotube and ZnO nanowires/microwires. This is a novel discovery of the piezotronic performance of $ZnSnO_3$ nanowires/microwires and their application in strain sensors.

EXPERIMENTAL METHODS

Material Synthesis. The source materials of Zn/Sn with ~1:1 in weight percentage (wt %) were placed on an alumina boat in a quartz reactor, and 50–100% (wt %) of graphite powder was added to induce a carbon thermal process. The synthesized temperature and working pressure were maintained at 900 °C and 10–50 Torr for 3 h, respectively. After that, as-synthesized products were subjected to an annealing process to increase the nanowires' dimension. The ultralong (~300–1000 μm) microwires were used to manipulate the microwires on a flexible polystyrene substrate (PS, 1 mm in thickness, 40 mm in length, and 10 mm in width). Both ends of the single microwire were bonded with the metal wire on the substrate, using silver paste for electrical measurement. The polydimethylsiloxane (PDMS) was used to package the devices to keep them robust during measurement.

Morphology and Structural Material. Material characterizations were performed using a field emission scanning electron microscope (FESEM, HITACHI S4800, operated at 3 kV), multipurpose thin-film X-ray diffractometer (Bruker, D8 SSS), and high-resolution transmission electron microscope (HRTEM, JEOL JEM-3000F, operated at 300 kV).

Electrical Measurement. The sensor was measured using Keithley 4200 and Stanford Research System Model DS 345 (30 MHz synthesized function generator).

Conflict of Interest: The authors declare no competing financial interest.

Acknowledgment. The authors would like to thank the support from National Science Council of the Republic of China (100-2918-I-035-003 and NSC 100-2628-E-035-006-MY2), BES DOE, and NSF.

Supporting Information Available: The contents of supporting information include S1–S3 and time-dependent decay data. This material is available free of charge *via* the Internet at http://pubs.acs.org.

REFERENCES AND NOTES

1. Zylberberg, J.; Belik, A. A.; Takayama-Muromachi, E.; Ye, Z. G. Bismuth Aluminate: A New High-Tc Lead-Free Piezo-/Ferroelectric. *Chem. Mater.* **2007**, *19*, 6385–6390.
2. Zeches, R. J.; Rossell, M. D.; Zhang, J. X.; Hatt, A. J.; He, Q.; Yang, C.-H.; Kumar, A.; Wang, C. H.; Melville, A.; Adamo, C.; *et al.* A Strain-Driven Morphotropic Phase Boundary in $BiFeO_3$. *Science* **2009**, *326*, 977–980.
3. Pan, C. F.; Li, Z. T.; Guo, W. X.; Zhu, J.; Wang, Z. L. Fiber-Based Hybrid Nanogenerators for/as Self-Powered Systems in Biological Liquid. *Angew. Chem., Int. Ed.* **2011**, *50*, 11192–11196.
4. Wang, Z. L.; Yang, R. S.; Zhou, J.; Qin, Y.; Xu, C.; Hu, Y. F.; Xu, S. Lateral Nanowire/Nanobelt Based Nanogenerators, Piezotronics and Piezo-Phototronics. *Mater. Sci. Eng. R* **2010**, *70*, 320–329.
5. Wang, Z. L. Piezopotential Gated Nanowire Devices: Piezotronics and Piezo-Phototronics. *Nano Today* **2010**, *5*, 540–552.
6. Wang, X. D.; Zhou, J.; Song, J. H.; Liu, J.; Xu, N. S.; Wang, Z. L. Piezoelectric Field Effect Transistor and Nanoforce Sensor Based on a Single ZnO Nanowire. *Nano Lett.* **2006**, *6*, 2768–2772.
7. Yang, Y.; Guo, W. X.; Zhang, Y.; Ding, Y.; Wang, X.; Wang, Z. L. Piezotronic Effect on the Output Voltage of P3HT/ZnO Micro/Nanowire Heterojunction Solar Cells. *Nano Lett.* **2011**, *11*, 4812–4817.

8. Yang, Q.; Wang, W. H.; Xu, S.; Wang, Z. L. Enhancing Light Emission of ZnO Microwire-Based Diodes by Piezo-Phototronic Effect. *Nano Lett.* **2011**, *11*, 4012–4017.
9. Yang, R. S.; Qin, Y.; Dai, L. M.; Wang, Z. L. Power Generation with Laterally Packaged Piezoelectric Fine Wires. *Nat. Nanotechnol.* **2009**, *4*, 34–39.
10. Zhou, J.; Gu, Y. D.; Fei, P.; Mai, W. J.; Gao, Y. F.; Yang, R. S.; Bao, G.; Wang, Z. L. Flexible Piezotronic Strain Sensor. *Nano Lett.* **2008**, *8*, 3035–3040.
11. Maeder, M. D.; Damjanovic, D.; Setter, N. Lead Free Piezoelectric Materials. *J. Electroceram.* **2004**, *13*, 385–392.
12. Mizoguchi, H.; Woodward, P. M. Electronic Structure Studies of Main Group Oxides Possessing Edge-Sharing Octahedra: Implications for the Design of Transparent Conducting Oxides. *Chem. Mater.* **2004**, *16*, 5233–5248.
13. Wang, H.; Huang, H. T.; Wang, B. A. First-Principles Study of Structural, Electronic, and Optical Properties of $ZnSnO_3$. *Solid State Commun.* **2009**, *149*, 1849–1852.
14. Nakayama, M.; Nogami, M.; Yoshida, M.; Katsumata, T.; Inaguma, Y. First-Principles Studies on Novel Polar Oxide $ZnSnO_3$, Pressure-Induced Phase Transition and Electric Properties. *Adv. Mater.* **2010**, *22*, 2579–2582.
15. Zhang, J.; Yao, K. L.; Liu, Z. L.; Gao, G. Y.; Sun, Z. Y.; Fan, S. W. First-Principles Study of the Ferroelectric and Nonlinear Optical Properties of the $LiNbO_3$-Type $ZnSnO_3$. *Phys. Chem. Chem. Phys.* **2010**, *12*, 9197–9204.
16. Gou, H. Y.; Gao, F. M.; Zhang, J. W. Structural Identification, Electronic and Optical Properties of $ZnSnO_3$: First Principle Calculations. *Comput. Mater. Sci.* **2010**, *49*, 552–555.
17. Kingon, A. I.; Srinivasan, S. Lead Zirconate Titanate Thin Films Directly on Copper Electrodes for Ferroelectric, Dielectric and Piezoelectric Applications. *Nat. Mater.* **2005**, *4*, 233–237.
18. Inaguma, Y.; Yoshida, M.; Katsumata, T. A Polar Oxide $ZnSnO_3$ with a $LiNbO_3$-Type Structure. *J. Am. Chem. Soc.* **2008**, *130*, 6704–6705.
19. Dal Corso, A.; Posternak, M.; Resta, R.; Baldereschi, A. *Ab Initio* Study of Piezoelectricity and Spontaneous Polarization in ZnO. *Phys. Rev. B* **1994**, *50*, 10715–10721.
20. Bernardini, F.; Fiorentini, V.; Vanderbilt, D. Spontaneous Polarization and Piezoelectric Constants of III−V Nitrides. *Phys. Rev. B* **1997**, *56*, 10024–10027.
21. Zhou, J.; Fei, P.; Gu, Y. D.; Mai, W. J.; Gao, Y. F.; Yang, R.; Bao, G.; Wang, Z. L. Piezoelectric-Potential-Controlled Polarity-Reversible Schottky Diodes and Switches of ZnO Wires. *Nano Lett.* **2008**, *8*, 3973–3977.
22. Hoel, C. A.; Amores, J. M. G.; Moran, E.; Alario-Franco, M. A.; Gaillard, J. F.; Poeppelmeier, K. R. High-Pressure Synthesis and Local Structure of Corundum-Type $In_{2-2x}Zn_xSn_xO_3$ ($x \leq 0.7$). *J. Am. Chem. Soc.* **2010**, *132*, 16479–16487.
23. Soutas-Little, R. W. *Elasticity*; Dover Publications: Mineola, NY, 1999; Vol. XVI, p 431.
24. Gao, Y.; Wang, Z. L. Electrostatic Potential in a Bent Piezoelectric Nanowire. The Fundamental Theory of Nanogenerator and Nanopiezotronics. *Nano Lett.* **2007**, *7*, 2499–2505.
25. Zhang, J.; Xu, B.; Qin, Z.; Li, X. F.; Yao, K. L. Ferroelectric and Nonlinear Optical Properties of the $LiNbO_3$-Type $ZnGeO_3$ from First-Principles Study. *J. Alloys Compd.* **2012**, *514*, 113–119.
26. Shao, Z. Z.; Wen, L. Y.; Wu, D. M.; Zhang, X. A.; Chang, S. L.; Qin, S. Q. Influence of Carrier Concentration on Piezoelectric Potential in a Bent ZnO Nanorod. *J. Appl. Phys.* **2010**, *108*, 124312–5.
27. Zhang, Y.; Liu, Y.; Wang, Z. L. Fundamental Theory of Piezotronics. *Adv. Mater.* **2011**, *23*, 3004–3013.
28. Wang, Z. L.; Song, J. H. Piezoelectric Nanogenerators Based on Zinc Oxide Nanowire Arrays. *Science* **2006**, *312*, 242–246.
29. Yang, Q.; Guo, X.; Wang, W. H.; Zhang, Y.; Xu, S.; Lien, D. H.; Wang, Z. L. Enhancing Sensitivity of a Single ZnO Micro-/Nanowire Photodetector by Piezo-Phototronic Effect. *ACS Nano* **2010**, *4*, 6285–6291.
30. Wang, Z. L. Toward Self-Powered Sensor Networks. *Nano Today* **2010**, *5*, 512–514.
31. Hsu, R.; Maslen, E. N.; duBoulay, D.; Ishizawa, N. Synchrotron X-ray Studies of $LiNbO_3$ and $LiTaO_3$. *Acta Crystallogr., Sect. B* **1997**, *53*, 420–428.